

Gustavo R. S. Assi¹

Assistant Professor
Department of Naval Architecture
and Ocean Engineering,
University of São Paulo,
São Paulo 05508-030, Brazil
e-mail: g.assi@usp.br

Guilherme S. Franco

Department of Naval Architecture
and Ocean Engineering,
University of São Paulo,
São Paulo 05508-030, Brazil

Michaelli S. Vestri

Department of Naval Architecture
and Ocean Engineering,
University of São Paulo,
São Paulo 05508-030, Brazil

Investigation on the Stability of Parallel and Oblique Plates as Suppressors of Vortex-Induced Vibration of a Circular Cylinder

Experiments have been carried out with models of free-to-rotate parallel and oblique plates fitted to a rigid section of circular cylinder to investigate the effect of plate length and oblique angle on the stability of this type of vortex-induced vibration (VIV) suppressor. Measurements of the dynamic response and trajectories of motion are presented for models with low mass and damping which are free to respond in the cross-flow and streamwise directions. It is shown that, depending on a combination of some geometric parameters, the devices might not be able to completely suppress VIV for the whole range of reduced velocities investigated. Plates with larger oblique angles turned to be less stable than parallel plates and induced high-amplitude vibrations for specific reduced velocities. Systems may present streamwise vibration due to strong flow separation and reattachment on the outer surface of plates with large oblique angles. Large angles may also increase drag. Experiments with a plain cylinder in the Reynolds number range from 3000 to 20,000 have been performed to serve as reference. Reduced velocity was varied between 2 and 13. Two-dimensional numerical simulation of static systems at $Re = 10,000$ revealed that complex and fully separated flow regimes exist for almost all investigated cases. There is a good chance that systems with such geometric characteristics will be unstable unless other structural parameters are positively verified. [DOI: 10.1115/1.4027789]

Keywords: VIV suppression, stability, free-to-rotate suppressors, parallel and oblique plates

1 Introduction

This paper reports on new fundamental studies regarding a pair of free-to-rotate plates acting as suppressors for the VIV of a circular cylinder. The development of new suppressors of flow-induced vibration (FIV) of offshore structures is a topic that became frequent in the literature in the past years. As previously discussed in Refs. [1–3], with the advancement of offshore oil exploration, research on FIV suppressors was pushed to a new level. “The industry demands suppressors that are not only efficient for low mass-damping systems but also that could be installed under harsh environmental conditions; such is the case for offshore risers” [3].

The present work contributes to the understanding of the dynamic stability and hydrodynamic phenomena behind a type of free-to-rotate device made of a pair of rigid plates attached to a cylinder. Suppressors employing parallel plates are already available as viable commercial solutions [4,5] for offshore drilling risers. Drilling risers are not in operation for as long as production risers; therefore, fatigue damage is not as important a concern as the loads caused by strong currents. Therefore, besides suppressing FIV, suppressors must contribute to reduce drag, consequently reducing pipe bend during drilling operation. A real drilling riser in the field is not a rigid structure, but responds the flow excitation in several modes of vibration with different frequencies. Testing free-to-rotate devices on a rigid section of a finite cylinder, as is the case in this fundamental investigation, elucidates the local fluid–structure interaction associated with the suppression

mechanism occurring in different sections along the riser, but is limited to capture the complex three-dimensional phenomena along the pipe. Small variations in the angle between the plates may affect the flow behavior around the suppressor, enhancing efficiency in suppression and potentially drag reduction. However, an opposite effect may also occur and plates with oblique angles may produce hydrodynamically unstable systems. The present study sets out to investigate these possibilities.

It is known that free-to-rotate suppressors may experience hydrodynamic instabilities that will not only cause a substantial increase in drag but also prevent it from suppressing vibrations [1]. Actually, an unstable free-to-rotate suppressor may induce the structure into more vigorous vibrations excited by a type of flutter mechanism. Assi et al. [1,3] have shown that the instability of free-to-rotate suppressors is directly related to the level of rotational resistance encountered in the system as well as geometric parameters such as plate length. They performed experiments in laboratory scale and showed that a free-to-rotate suppressor formed by a single splitter plate may need a minimum rotational resistance (or be above a critical rotational friction) to enable a stable configuration with effective suppression. The same was verified for free-to-rotate suppressors composed of two parallel plates [6], revealing that a minimum rotational resistance is necessary to stabilize the devices.

Assi et al. [1,2] have already shown that 1D-long parallel plates can be very efficient in suppressing both VIV and wake-induced vibration (WIV). WIV occurs when the downstream body of a set is excited by the unsteady wake generated from another body placed upstream [7,8]. In the present work, we set out to investigate if free-to-rotate oblique plates are able to find stable configurations and suppress VIV for various plate lengths and oblique angles. The installation of free-to-rotate suppressors on offshore risers requires fitting bearings or sliding components around the

¹Corresponding author.

Contributed by the Ocean, Offshore, and Arctic Engineering Division of ASME for publication in the JOURNAL OF OFFSHORE MECHANICS AND ARCTIC ENGINEERING. Manuscript received September 26, 2013; final manuscript received May 23, 2014; published online June 19, 2014. Assoc. Editor: Antonio C. Fernandes.

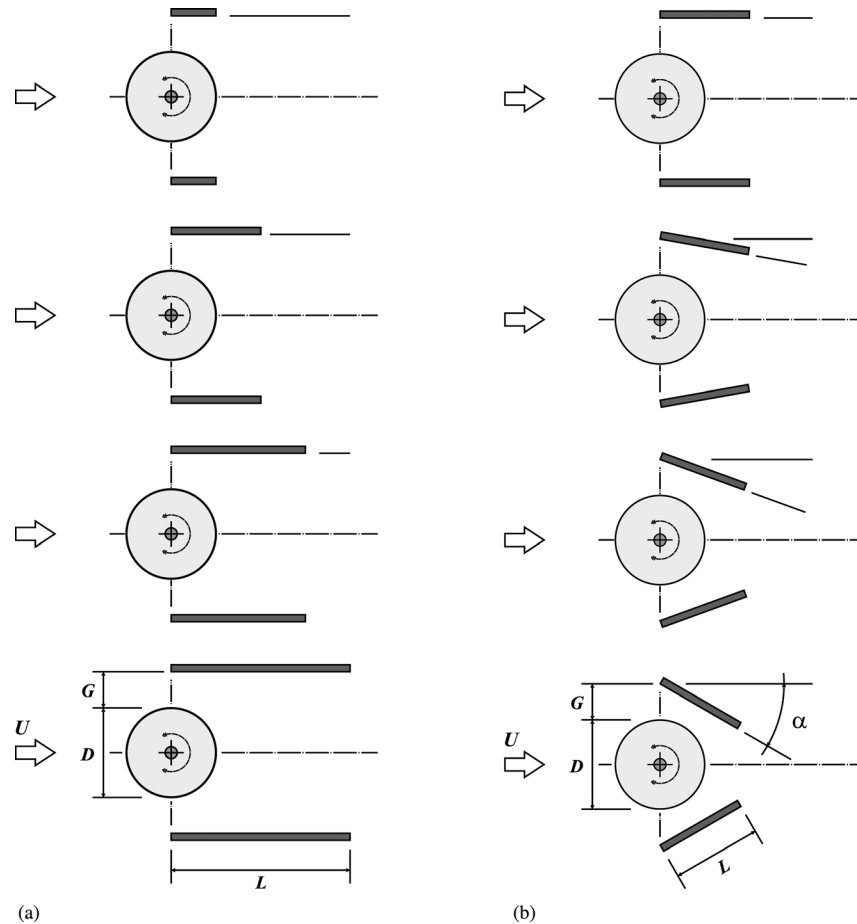


Fig. 1 (a) First experiment: Free-to-rotate parallel plates. Fixed $G/D=0.4$ and $\alpha=0$ deg, varying $L/D=0.5, 1.0, 1.5$, and 2.0 from top to bottom. (b) Second experiment: Free-to-rotate oblique plates. Fixed $G/D=0.4$ and $L/D=1.0$, varying $\alpha=0$ deg, 10 deg, 20 deg, and 30 deg from top to bottom.

pipe that may be vulnerable to fatigue or deteriorate due to the marine environment. The present study is limited to a fundamental investigation of a concept as far as the stability of the system is concerned; hence, it will not discuss the devices in a deeper technological level.

2 Parallel and Oblique Plates

Variations on the concept of double plates, some inspired by the early work of Grimmering [9] related to suppressing VIV of submarine periscopes, were the inspiration for previous works that employed a similar apparatus [1–3,6,10,11]. In Grimmering's experiments, the plates were fixed since the direction of the flow around a submarine is known, but in the investigations mentioned above the plates were free to rotate according to the flow orientation.

Based on the previous investigations [1], we believe that parallel plates and splitter plates are able to suppress VIV based on the same fluid-dynamic mechanism. Free-to-rotate parallel plates are not a "fairing" in the strict sense of the term, i.e., they do not make the cylinder a streamlined body. For this to occur, the length of the fairing would have to be many times the diameter of the cylinder (as shown in Refs. [12–14]). In essence, parallel plates act in the near wake with fully separated flow, avoiding the interaction between the shear layers and delaying vortex formation and shedding, hence the same mechanism as splitter plates and short-tail (or teardrop) fairings [1,3].

In a previous work [6], we have investigated if free-to-rotate parallel plates would be able to find stable configurations and suppress VIV for various plate lengths. In that configuration, the

leading edge of the plate was practically touching the cylinder wall, creating a chamber of almost stagnant flow downstream of the cylinder and in between the plates. That configuration did not allow any flow to "ventilate" the near wake. The longer the plates, the larger would become the region of stagnant flow. In the present study, we want to investigate if a small vent in the form of a gap between the plates and the cylinder would possibly allow high-speed flow to feed momentum into the near wake, creating a more streamlined body by disrupting the interaction between the shear layers that generate vortices.

We chose to vary three geometric parameters to characterize the suppressors, as seen in Figs. 1(a) and 1(b): Plate length normalized by the diameter, L/D ; plate angle, α , that defines the oblique configurations ($\alpha=0$ deg means parallel plates); and the normalized gap, G/D , measured between the leading edge of the plate and the cylinder wall. Both plates are installed so that their leading edge is aligned with the center of the cylinder. Plates cannot move in relation to each other, but the pair is free to rotate about the center of the cylinder. Plate thickness $t/D=0.06$ was kept constant in the present study, even though it was thought to be a relevant parameter for investigation.

It is intuitive to think that if we held L/D fixed, only varying the other two geometrical parameters, we could already produce several different flow patterns. G/D is directly related to the flow intake into the near wake, especially related to the flow behavior in the boundary layers. Increasing α directs momentum inward (toward the centerline), but it is also directly related to strong flow separation that may occur on the outer surface of the plates. Minor variations in both G and α would be enough to modify the flow behavior. Actually, it is not difficult to imagine that an optimum

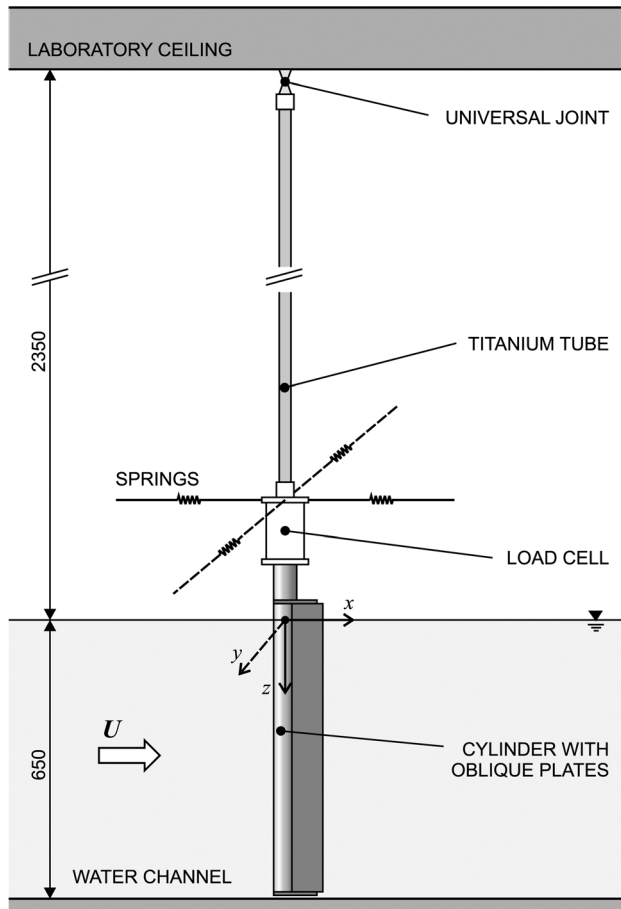


Fig. 2 Experimental setup: cylinder with parallel plates mounted on the two-degrees of freedom rig in the test section of the NDF-USP water channel

solution to minimize vibration and reduce drag would have a small gap and a minute oblique angle with almost no separation.

The present investigation is not intended as a study of optimization, but it aims on the understanding of the overall behavior of the system for larger variations of G/D , L/D , and α , much larger than the intuitive geometries. At the moment, we are more concerned with the overall stability of the system rather than with optimum proportions. Therefore, our parameters will vary in large steps as follows: $L/D = 0.5, 1.0, 1.5, 2.0$ and $\alpha = 0^\circ, 10^\circ, 20^\circ, 30^\circ$ with $G/D = 0.4$ kept constant. Overall, our broader study results from 80 different tested configurations. This paper will focus on the eight most interesting cases, not necessarily the ones that produced effective suppression and drag reduction, but especially on those that showed surprising results. The study was divided into two experiments. In the first experiment, with parallel plates shown in Fig. 1(a), $G/D = 0.4$ and $\alpha = 0^\circ$ were kept constant while L/D was varied in four steps. In the second experiment, with oblique plates shown in Fig. 1(b), $G/D = 0.4$ and $L/D = 1.0$ were kept constant while α was varied in four steps. Varying one parameter at a time was thought to help the parametric analysis that will follow.

3 Experimental Arrangement

Experiments have been carried out in the circulating water channel of NDF Fluids and Dynamics Research Group at the University of São Paulo, Brazil. The NDF-USP water channel has an open test section which is 0.7 m wide, 0.9 m deep, and 7.5 m long. Good quality flow can be achieved up to 1.0 m/s with turbulence intensity less than 3%. This laboratory has been especially

Table 1 Structural properties

	m^*	ζ (%)	$m^*\zeta$
Plain cylinder	1.90	0.2	0.0038
Cylinder with plates			
$L/D = 0.5$	2.10	0.2	0.0042
$L/D = 1.0$	2.17	0.2	0.0043
$L/D = 1.5$	2.24	0.2	0.0045
$L/D = 2.0$	2.30	0.2	0.0046

designed for experiments in FIV; further details about the facilities are described in Ref. [15].

A rigid section of circular cylinder with an external diameter of $D = 50$ mm was made of a perspex tube (please refer to Figs. 1 and 2 for details). Four pairs of rigid perspex plates were manufactured varying in length in four steps of $L/D = 0.5, 1.0, 1.5$, and 2.0 . The plates were mounted on ball bearings at the extremity of the cylinder and could not move in relation to each other, i.e., the angle between the plates was kept constant at all times. The leading edge was kept at the same vertical alignment as the center of the cylinder so that plates were oriented at the $\pm 90^\circ$ points in relation to the incoming flow. The oblique angle of the plates α in Fig. 1(b) (defined as the actual angle of attack for each flat plate) was adjusted in four steps of $\alpha = 0^\circ, 10^\circ, 20^\circ$, and 30° . As a result, the pair of parallel or oblique plates would freely rotate as one body around the center of the cylinder. The gap between the leading edge of the plates and the cylinder wall was kept constant at $G/D = 0.4$. As far as the boundary layer thickness is concerned, this is considered to be a large gap relative to the cylinder diameter, at least large enough for the plate not to interact with the laminar boundary layers around the natural separation points. A schematic representation of all the considered geometries is presented in Fig. 1. Rotational friction was not measured in this study, instead it was simply verified if the actual level of rotational friction in the bearings was high enough to stabilize the 1D-long plates around the expected peak of response for VIV.

Models were mounted on a low-damping rig that allowed the cylinder to freely respond in both cross-flow and streamwise directions, as seen in Fig. 2. The cylinder model was mounted at the lower end of a long titanium tube forming the arm of a rigid pendulum connected to a universal joint fixed at the ceiling of the laboratory. The water channel was filled up to 650 mm, resulting in a submerged length to diameter ratio of 13. The design and construction of the pendular elastic rig were made by Freire and Meneghini [16] based on a previous idea employed by Assi et al. [1,2] for experiments with VIV suppressors. Two independent optical sensors were employed to measure displacements in the x and y directions at the midlength of the model. It should be noted that for a displacement equal to one diameter the inclination angle of the cylinder was only just over 1 deg from the vertical. Two pairs of springs were installed in the x and y axes to set the natural frequencies in both directions of motion. The springs were chosen to provide the same natural frequency (f_0) measured in air in both the cross-flow and streamwise directions.

Decay tests have been performed in air in order to determine the natural frequencies of the system in both direction as well as the level of structural damping. The apparatus with one universal joint and four springs turned out to present a very low structural damping of $\zeta = 0.20\%$, measured as a fraction of the critical damping. The total oscillating mass of the system was measured in air, resulting in a nondimensional mass parameter of $m^* \approx 2.0$, defined as the ratio between the total mass and the mass of displaced fluid. Consequently, the mass-damping parameter $m^*\zeta$ of the system was kept to the lowest possible value in order to amplify the amplitude of response. Preliminary tests have been performed with a plain cylinder to serve as reference for comparison. Table 1 summarizes the structural parameter for both the plain cylinder and the cylinders fitted with plates of various

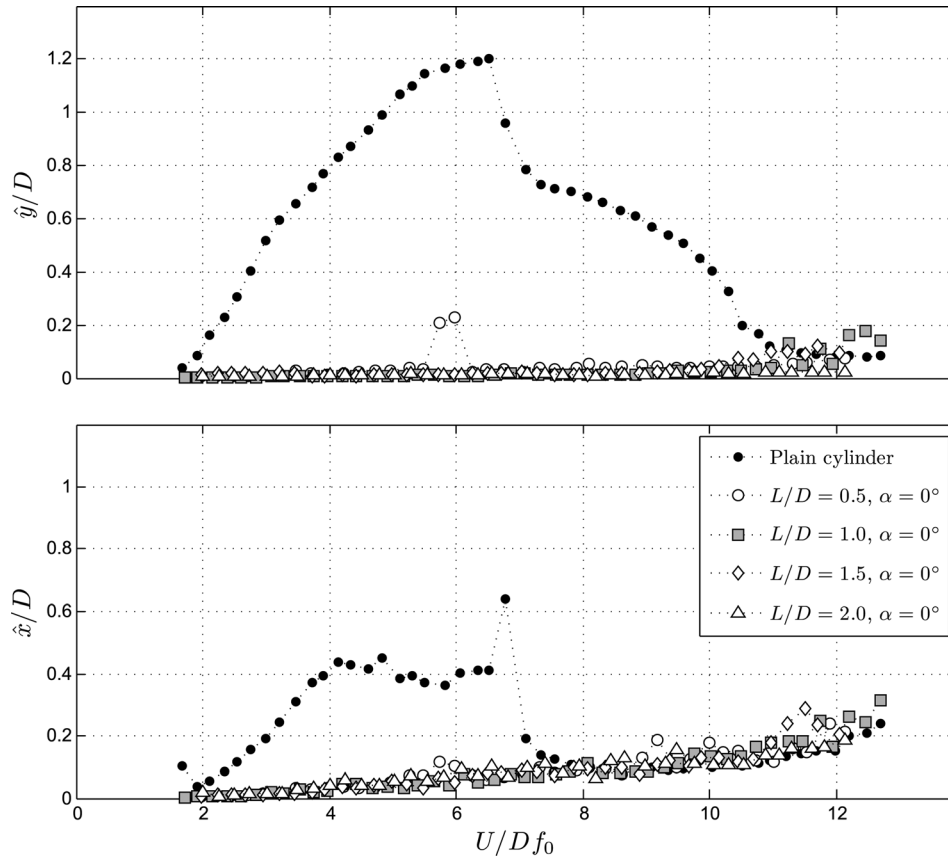


Fig. 3 First experiment: cross-flow (\hat{y}/D) and streamwise (\hat{x}/D) amplitude of vibration versus reduced velocity for a plain cylinder compared to cylinders fitted with parallel plates of various lengths

lengths. Notice that m^* varies slightly from model to model due to the mass variation of the installed plates.

Measurements were made using a fixed set of springs and the reduced velocity range covered was up to 13, where reduced velocity, U/Df_0 , is defined using the cylinder natural frequency of oscillation in the cross-flow direction measured in air. The only flow variable changed during the course of the experiments was the flow velocity, U , which alters both the reduced velocity and the Reynolds number between 3000 and 20,000. Throughout the present study, cylinder displacement amplitudes nondimensionalized by the plain cylinder diameter (\hat{x}/D for streamwise and \hat{y}/D for cross-flow directions) were found by measuring the root mean square value of response and multiplying by the square root of 2 (the so called equivalent harmonic amplitude). This is likely to give an underestimation of maximum response but was judged to be perfectly acceptable for assessing the effectiveness of VIV suppression devices.

4 Preliminary Results for a Plain Cylinder

A preliminary VIV experiment was performed with a plain cylinder in order to validate the setup and methodology. The same pendulum rig was employed, only replacing the model with parallel plates by a plain cylinder with the same diameter. Figures 3 and 4 will compare the reference cross-flow and streamwise responses obtained for the plain cylinder with those obtained for each suppression device. As far as the plain cylinder is concerned, the observed peak amplitude of $\hat{y}/D = 1.2$ between $U/Df_0 = 6.0$ and 7.0 is in good agreement with other results presented in the literature [1,17]. The general behavior of the cross-flow response confirms the typical response for the two-degrees of freedom VIV of a system with the same natural frequency in both directions.

The recorded streamwise response presented a peculiar feature. Around reduced velocity of 7.0, corresponding to the transition from the upper to the lower branch in the cross-flow response, we observed high-amplitude vibration above $\hat{x}/D = 0.6$. At first sight, one might conclude that such a distinct peak could be related to a local resonance between the streamwise excitation and a higher harmonic in that direction. However, this idea was discarded once the time series for the displacement signal was analyzed. In fact, it occurred that the cylinder experienced an unstable transition from the upper to the lower branch in the cross-flow oscillations, jumping back and forth from one mode to the other. This alternation between two different levels of amplitude had an effect on the streamwise response due to fluctuations on the mean drag induced by the cross-flow vibrations. As a result, the response appeared as if the cylinders were oscillating with $\hat{x}/D > 0.6$ around a mean position, but in fact it was alternating between two branches of vibration as long as the transition was not completed.

Although the cylinder was initially aligned in the vertical position, in flowing water, the mean drag displaces the cylinder from its original location reaching a slightly inclined configuration from the vertical. This was judged not to be detrimental to the experiment, hence the inclination of the cylinder was not corrected between each step of increasing flow speed. The same procedure was adopted for the cylinders fitted with plates.

5 Results for Cylinders With Plates

Figures 3 and 4 also present two sets of data with cross-flow and streamwise response curves for the suppressors tested in the first and second experiments, respectively. We shall start discussing results from the first experiment.

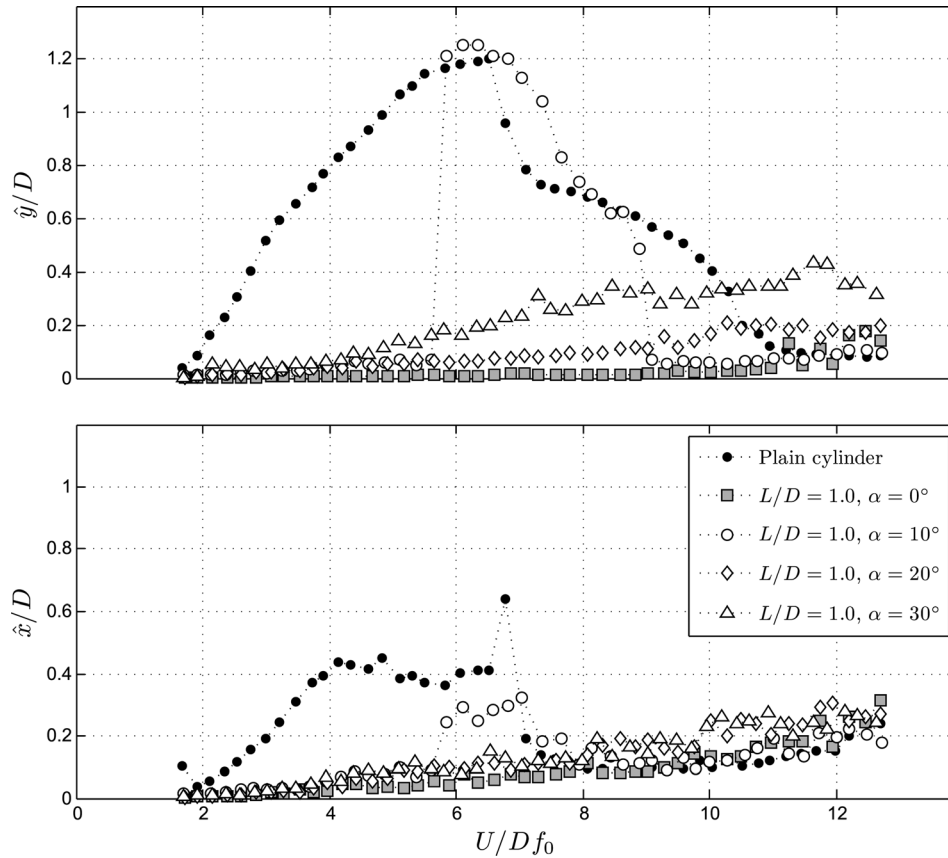


Fig. 4 Second experiment: cross-flow (\hat{y}/D) and streamwise (\hat{x}/D) amplitude of vibration versus reduced velocity for a plain cylinder compared to cylinders fitted with oblique plates of various angles

5.1 First Experiment: Varying L/D . The first experiment presents only parallel plates varying in length. These configurations differ from those of Assi et al. [6] in the existence of a lateral gap of $G/D = 0.4$ between the cylinder and the plate; nevertheless, the overall behavior of the free-to-rotate devices is very similar in both studies. The general behavior of all free-to-rotate parallel plates shows a remarkable reduction in vibration in both directions for most of the reduced velocity range investigated (Fig. 3). Given the minimum level of rotational friction provided by the bearings, all parallel plates were found to be reasonably stable for the whole range of reduced velocities.

Except for two data points for the shorter plates of $L/D = 0.5$ around reduced velocity of 6.0, most plates were able to practically mitigate vibrations below $\hat{y}/D = 0.2$ for the whole range of reduced velocities, even during the cross-flow and streamwise resonances. This localized amplification of the response around $U/Df_0 = 6.0$ is attributed to a minor resonance of the vortex-shedding mechanism altered by the presence of the short plates. For reduced velocities greater than ten, random vibration associated with turbulence buffeting appeared for all suppressors as well as for the plain cylinder, reaching $\hat{y}/D \approx 0.1$. The increase of amplitude is even more pronounced for the streamwise motion, monotonically building up from reduced velocity of 8.0 and reaching $\hat{x}/D \approx 0.3$ for the maximum flow speed. A qualitative analysis of trajectory plots (Fig. 6) reveals a nonperiodic motion, supporting the buffeting hypothesis. We shall return to this point when discussing the trajectories in Sec. 6.

Based on the first experiment, we cannot tell which plate length presented the most efficient suppression. We cannot affirm that all plates are perfectly stable either, since we have observed some distinct vibration for $L/D = 0.5$. One can only infer that shorter plates around $L/D = 0.5$ may be more prone to instability than the others. There is a possibility that other plates may present

unstable regimes as well, especially if plate length is increased beyond $L/D = 2.0$. Results obtained for the 1D-long parallel plates are in good agreement with the previous experiments reported by Assi et al. [1,10,11]. Although their parallel plates had a slightly different geometry than the ones tested in this experiment, the general behavior agrees quite well.

Assi et al. [6] showed that parallel plates with no gap ($G/D = 0.0$) were able to suppress VIV because they inhibited the interaction between the free shear layers, delaying vortex formation and consequent excitation. For a geometry with $G/D = 0.0$, the boundary layers do not separate, but the shear layers flow alongside the outer surface of the plates. Now, in the present study with a large gap of $G/D = 0.4$, the flow separates around the cylinder and the free shear layers flow downstream along the inner side of the parallel plates. Hence, there is no obstruction to the interaction of the shear layers and, in principle, the vortex-shedding mechanism occurs confined in between the plates. Even with vortices being shed in between the plates, VIV is still suppressed by parallel plates with $G/D = 0.4$.

5.2 Second Experiment: Varying α . The second experiment presents 1D-long plates varying only the oblique angle α . These are new results for which we found no references in the literature to be compared with. Case $L/D = 1.0$ and $\alpha = 0$ deg (marked with gray squares in Figs. 3 and 4) is repeated in both experiments. Differently from the first experiment, variation in α showed an interesting effect over the response, especially in the cross-flow displacement of the cylinder. As seen, $\alpha = 0$ deg suppressed vibration below $\hat{y}/D = 0.1$ for most of the velocity range tested. Now, as α is increased in steps of 10 deg the cross-flow response curves reach higher levels of monotonically increasing amplitude.

The only exception was found for the case for $\alpha = 10$ deg in which the system presented resonant behavior for reduced

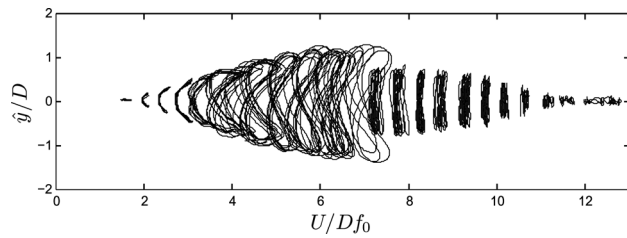


Fig. 5 Reference experiment: trajectories of motion for a plain cylinder

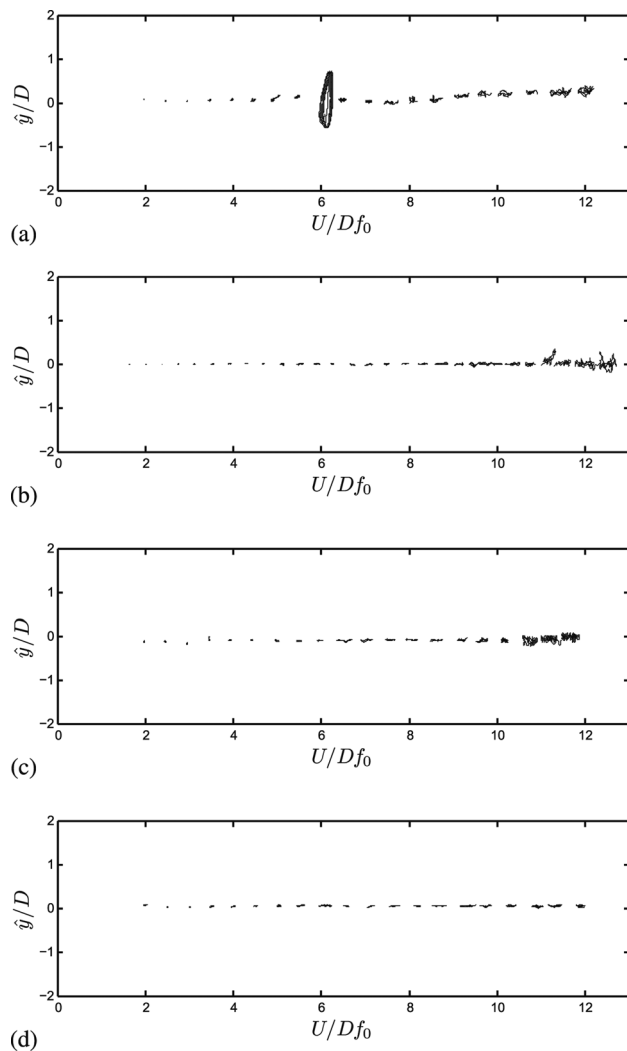


Fig. 6 First experiment: trajectories of motion for a cylinder fitted with parallel plates of different lengths

velocities between 6.0 and 9.0. During this interval, the amplitude of response practically followed the response curve obtained for a plain cylinder reaching almost $\hat{y}/D = 1.3$ for reduced velocity of 6.0. At the same time, streamwise vibration was also increased to $\hat{x}/D \approx 0.3$ for a shorter resonant range between reduced velocities of 6.0 and 7.0. Periodic motion registered in the trajectory plot of Fig. 7(b) supports the hypothesis of resonant vibration within a limited range of reduced velocity. Apart from that, all other cases showed vibration that is associated with turbulence buffeting rather than a resonant phenomenon such as VIV. Of course, other excitation mechanisms may also be occurring for highly oblique

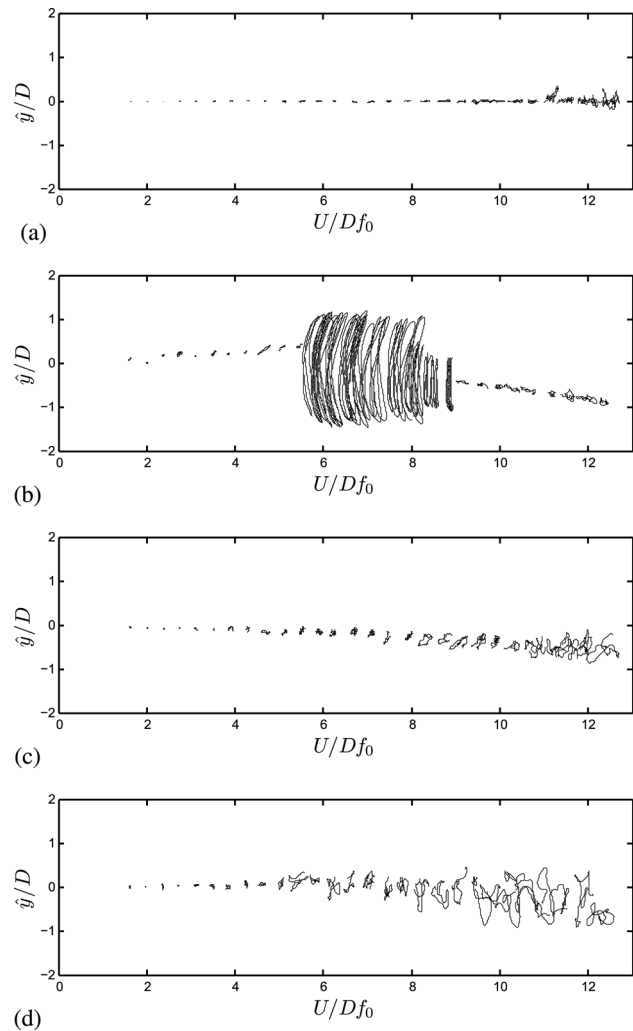


Fig. 7 Second experiment: trajectories of motion for a cylinder fitted with oblique plates of different angles

plates. It is not difficult to imagine that large values of α generate strong separated flow around the plates and the cylinder. The interaction between unstable reattachment bubbles and small-scale vortices may be driving the cylinder into vibrations of a different nature. Minute variations of α may drastically alter the flow behavior in the region in between the plates. It is interesting to know if there is a value of α (as well as the other geometric parameters) to permit maximum “ventilation” of the near wake with minimum flow separation around the plates and consequent VIV suppression with drag reduction.

6 Trajectories of Motion

Trajectory figures are a simple and qualitative manner to analyze the responses presented in Figs. 3 and 4. Samples of displacement trajectories obtained for the plain cylinder (Fig. 5) are compared with those for the suppressors for the first and second experiments (Figs. 6 and 7). The same scale was kept in all figures to allow for direct comparison between them and a few trajectory lines have been suppressed for clarity. The plain cylinder response in Fig. 5 presents characteristic figures typical of VIV in two degrees of freedom. A C-shaped trajectory, at the initial branch, progressively changes into an eight-shaped trajectory up to the peak amplitude at the upper branch. When the response changes from the upper to the lower branch, after reduced velocity of 6.0, the trajectories immediately take a flatter shape with reduced displacement in the streamwise direction.

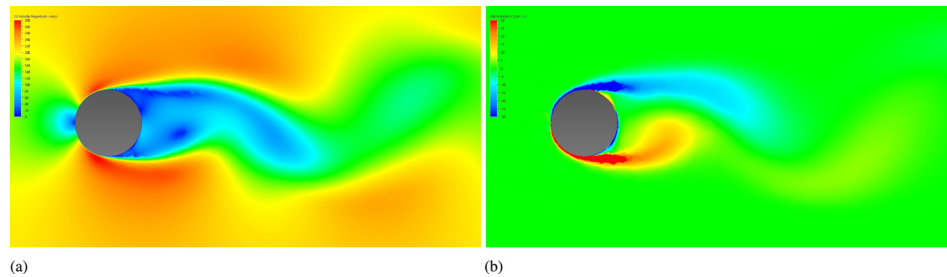


Fig. 8 Reference simulation: wake of a plain cylinder

Trajectories for the suppressors investigated in both experiments are very different from those of the plain cylinder in Fig. 5. In general terms, the cylinders fitted with free-to-rotate plates present small movement around a mean position for most of the reduced velocity range, except for a few points as seen in Figs. 6(a) and 7(b). A distinct behavior was observed for a parallel plate with $L/D = 0.5$ around reduced velocity 6.0, as seen in Fig. 6(a) and registered in Fig. 3. Sometimes, the plates were unable to stabilize for a range of reduced velocities and periodic vibrations were registered for a few cycles, as illustrated in Fig. 4 for $L/D = 1.0$, $\alpha = 10$ deg and reduced velocity between 6.0 and 9.0. Such vibrations are normally associated with resonant mechanisms, such as VIV, but they can also be an effect of a flutter type of excitation due to the rotational movement of the plate.

Almost all trajectory plots of Figs. 6 and 7 show random vibrations for the higher reduced velocities. Figure 7(d) particularly shows nonperiodic vibrations for most of flow speeds. In addition, Figs. 7(b)–7(d) clearly show that the cylinder drifted to one side as the flow speed was increased. Oblique plates, especially those with high angles, tend to be more difficult to align with the flow, thus stabilizing at a small deflected position from the centerline. As a consequence, a steady lift force drives the cylinder toward the side the plate has deflected. Assi et al. [1,3] showed that such a drift is due to occur for a single splitter plate that finds a deflected but stable position to one of the sides while suppressing VIV. Assi et al. [6] showed a similar behavior for parallel plates longer than $L/D = 1.0$. Now, a similar behavior has been observed for oblique plates.

7 Numerical Simulations of the Flow

In order to gain insight into the flow around the cylinder and devices, numerical simulations have been performed for the four geometries of oblique plates investigated in the second experiment. Keeping $G/D = 0.4$ and $L/D = 1.0$ fixed, α was varied in the four steps studied above. Such numerical simulations are presented here to illustrate and contribute to our understanding of the flow characteristics around the devices. It is evident that the main body of work presented in this paper is concerned with the experimental results obtained for free-to-rotate systems. In the numerical study, the cylinder and the plates are all static, i.e., they cannot move in relation to one another nor can the system respond with FIV. Nevertheless, we believe that even a qualitative analysis of the flow around a static system is able to elucidate some interesting points.

The commercial code AUTODESK SIMULATION Computational Fluid Dynamics (CFD) was employed in the study. Each two-dimensional mesh was composed of around 8000 elements with particular care taken into refining the mesh around the walls and in the gap between the cylinder and the plates. The unsteady Reynolds-Averaged Navier–Stokes equations were solved for an incompressible flow employing a segregated upwind, finite element method. The two-dimensional domain extended for $5D$ upstream, $15D$ downstream, and $5D$ to each side of the cylinder. Reynolds number was set to 10,000 and the k- ω shear-stress transport (SST) turbulence model was employed. Each simulation

was performed for at least 100 cycles of vortex shedding after a steady wake regime had been reached.

The results discussed below focus on the vortex formation region and the near wake in order to observe flow structures around the plates and in the gap between plates and cylinder. Velocity and vorticity fields are both presented side by side for the same instant in time for each configuration. The flow around a single cylinder without plates has been computed as a reference and is presented in Fig. 8. As expected, a classic von Karman wake was obtained. The color scales for velocity magnitude and vorticity is the same in all figures to allow for direct comparison of the wakes.

Figure 9 presents the results for the cylinders fitted with plates. In Figs. 9(a) and 9(b), we observe that the two parallel plates spaced from the cylinder barely interfere with the vortex formation mechanism. A typical vortex wake is formed and confined between them, but only farther downstream the vorticity generated on the plates will interact with the vortices shed from the cylinder. The result is a rather typical vortex street with minor interference from the external vorticity from the plates. Nevertheless, even this minor effect might be responsible for the suppression achieved by this geometry through the whole range of reduced velocities, as observed in the experimental results in Fig. 7(a).

Once the oblique angles are changed, the flow around the cylinder and plates changes drastically. Figures 9(c) and 9(d) show that even the smallest angle of attack of $\alpha = 10$ deg already causes considerable separation of the flow on the outer surface of the plates. One may argue that $\alpha = 10$ deg is not a small angle of attack and one should not expect anything different from the separated flow around a flat plate; we agree with that. The vortex formation region is confined between the plates and forced toward the centerline by the high-speed flow coming through the gap. Vortices are shed with higher frequency in this narrower wake and then combined with other small vortices shed from the plates. The result is a periodic wake with a frequency signature different from the typical Strouhal number of a plain cylinder. Experimental results in Fig. 7(b) have shown that this configuration can become very unstable and induce severe vibrations to the level of the VIV response of a plain cylinder.

For $\alpha = 20$ deg, shown in Figs. 9(e) and 9(f), the high-speed flow ventilated through the gaps forces a much narrower wake behind the cylinder, with the contribution of the two plates closing the gap as the vortices are shed downstream. The overall wake is now dominated by the two large vortex systems shed from each of the oblique plates. They interfere further downstream merging with the small vortices formed behind the cylinder near the centerline.

The final configuration with $\alpha = 30$ deg, presented in Figs. 9(g) and 9(h), shows that the flow behavior has changed completely from a wake dominated by vortices shed from the cylinder to a wake dominated by vortices shed from the plates. While for $\alpha = 10$ deg and 20 deg, we could say that vortices from the cylinder and from the plates had roughly the same scale and intensity, we observe now for $\alpha = 30$ deg that the wake is completely dominated by vortices shed from the plates. The vortex formation region behind the cylinder is practically nonexistent and only a symmetrical bubble is observed to survive between the jets from

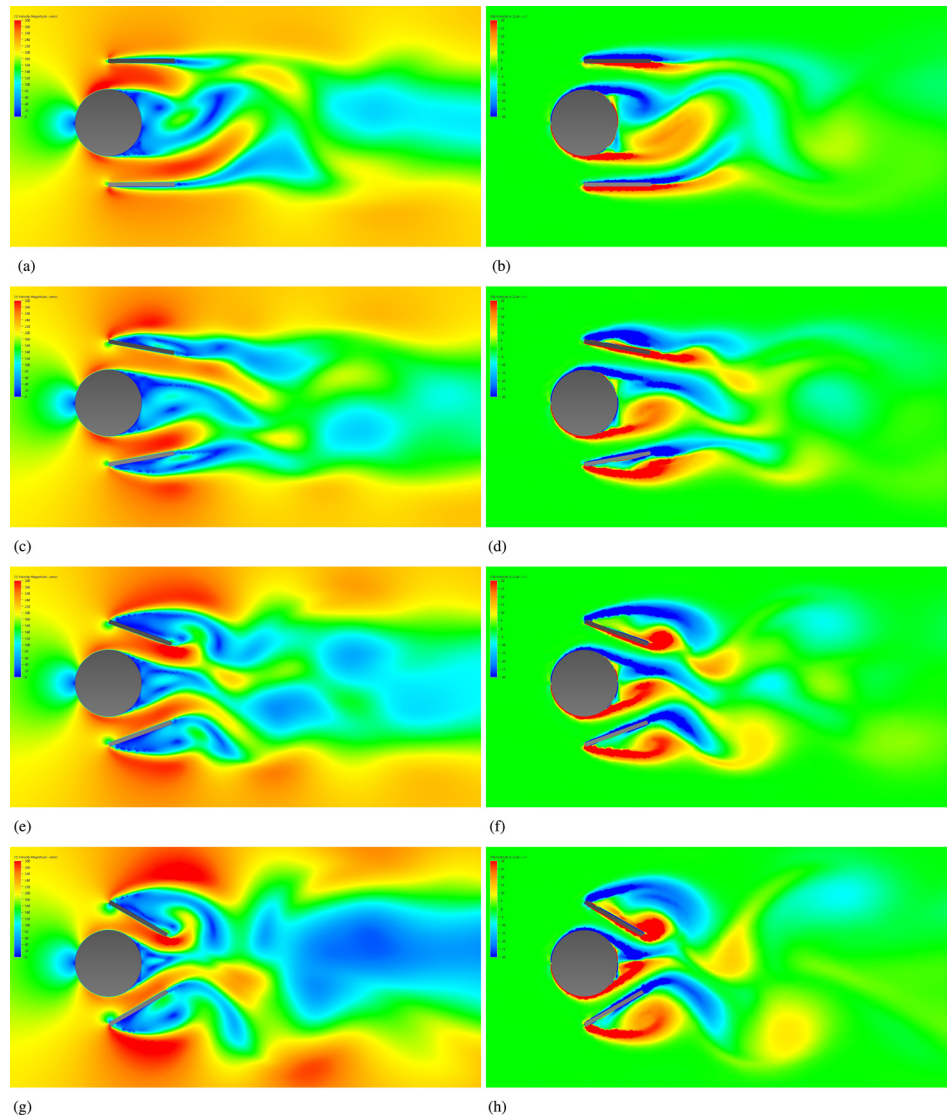


Fig. 9 Wake of a cylinder with oblique plates: fixed $G/D = 0.4$ and $L/D = 1.0$, varying $\alpha = 0$ deg, 10 deg, 20 deg, and 30 deg from top to bottom

the gaps through the confinement of the plates. The overall wake is a result of the interference of the wakes of mainly two bluff bodies, i.e., the plates.

Of course numerical simulations of this sort are very limited in modeling the fluid–structure interaction occurring in the free-to-rotate experiments. But it becomes clear that systems with so many regions of separated flow, with severe wake interactions and gaps with accelerated flow in the form of jets have all the ingredients to produce unstable dynamics. In fact, we can conclude that suppressors with such geometric characteristics will rarely help to streamline the flow around a cylinder; on the contrary, the system will behave as a distinct bluff body with several separation regions and wake interferences. Stability becomes very difficult to achieve with such configurations and will require other structural parameters such as damping and inertia to be precisely adjusted.

8 Conclusions

Although being a fundamental study in laboratory scale, the present investigation throws some light in the technological development of new geometries for VIV suppressors. Results showed that free-to-rotate parallel and oblique plates with $G/D = 0.4$ may present hydrodynamically unstable behavior depending on L/D and α . Nevertheless, most of the tested configurations were able to

suppress vibrations down to $\hat{y}/D \approx 0.2$ and $\hat{x}/D \approx 0.2$ for most of the reduced velocity range, given the level of rotational friction of the system. In summary, we conclude that:

- (i) The gap between plates and cylinder is thought to act as a vent, directing the flow toward the near wake and injecting momentum into the vortex formation region. However, large gaps, such as the one studied in the present paper, may cause the plate to act as a strong lifting surface detached from the cylinder.
- (ii) Systems may present streamwise vibration due to strong flow separation and reattachment on the outer surface of the plates, particularly for larger oblique angles. Consequently, large values of α also increase drag.
- (iii) An undesirable lateral force appeared to act on the system for plates with high oblique angles causing the cylinder to drift to one side. This is being caused by a small deflection of the plates (although such a deflection angle was too small to be noticeable or measured in the present work) or nonsymmetric flow separation around the cylinder.
- (iv) Numerical simulation of the flow around static systems revealed that complex and fully separated flow regimes exist for almost all investigated cases. The wake of the cylinder is severely affected by the wakes generated on the plates and the wake of a distinct bluff body is what

remains farther downstream. Systems with such flow characteristics will have a tendency to become unstable unless other structural parameters are adequately adjusted.

Acknowledgment

The authors wish to acknowledge the support of FAPESP São Paulo Research Foundation (No. 2011/00205-6). G.R.S.A. is thankful to CNPq (No. 308916/2012-3). G.S.F. is in receipt of a undergraduate research grant from ANP Agência Nacional do Petróleo, Gás Natural e Biocombustíveis (PRH-19).

Nomenclature

D = cylinder external diameter
 f_0 = natural frequency in air
 G = gap between plate edge and cylinder wall
 L = plate length
 m^* = mass ratio
 Re = Reynolds number
 U = flow speed
 U/Df_0 = reduced velocity
 \hat{x} = streamwise harmonic amplitude of vibration
 \hat{y} = cross-flow harmonic amplitude of vibration
 α = plate oblique angle
 ζ = structural damping ratio

References

- [1] Assi, G. R. S., Bearman, P. W., and Kitney, N., 2009, "Low Drag Solutions for Suppressing Vortex-Induced Vibration of Circular Cylinders," *J. Fluids Struct.*, **25**, pp. 666–675.
- [2] Assi, G. R. S., Bearman, P. W., Kitney, N., and Tognarelli, M., 2010, "Suppression of Wake-Induced Vibration of Tandem Cylinders With Free-to-Rotate Control Plates," *J. Fluids Struct.*, **26**, pp. 1045–1057.
- [3] Assi, G. R. S., Bearman, P. W., Rodrigues, J. R., and Tognarelli, M., 2011, "The Effect of Rotational Friction on the Stability of Short-Tailed Fairings Suppressing Vortex-Induced Vibrations," 30th International Conference on Ocean, Offshore and Arctic Engineering, *OMAE2011*, Rotterdam, The Netherlands, June 19–24.
- [4] Schaudt, K., Wajnikonis, C., Spencer, D., Xu, J., Leverette, S., and Masters, R., 2008, "Benchmarking of VIV Suppression Systems," 27th International Conference on Offshore Mechanics and Arctic Engineering, *OMAE2008*, Estoril, Portugal, June 15–20.
- [5] Taggart, S., and Tognarelli, M., 2008, "Offshore Drilling Riser VIV Suppression Devices? What is Available to Operators?," 27th International Conference on Offshore Mechanics and Arctic Engineering, *OMAE2008*, Estoril, Portugal, June 15–20.
- [6] Assi, G. R. S., Rodrigues, J. R., and Freire, C., 2012, "The Effect of Plate Length on the Behaviour of Free-to-Rotate VIV Suppressors With Parallel Plates," 31st International Conference on Ocean, Offshore and Arctic Engineering, *OMAE2012*, Rio de Janeiro, Brazil, July 1–6.
- [7] Assi, G. R. S., Bearman, P. W., and Meneghini, J. R., 2010, "On the Wake-Induced Vibration of Tandem Circular Cylinders: The Vortex Interaction Excitation Mechanism," *J. Fluid Mech.*, **661**, pp. 365–401.
- [8] Assi, G. R. S., Bearman, P. W., Carmo, B. S., Meneghini, J. R., Sherwin, S. J., and Willden, R. H. J., 2013, "The Role of Wake Stiffness on the Wake-Induced Vibration of the Downstream Cylinder of a Tandem Pair," *J. Fluid Mech.*, **718**, pp. 210–245.
- [9] Grimminger, G., 1945, "The Effect of Rigid Guide Vanes on the Vibration and Drag of a Towed Circular Cylinder," David Taylor Model Basin, Technical Report No. 504.
- [10] Assi, G. R. S., and Bearman, P. W., 2008, "VIV Suppression and Drag Reduction With Pivoted Control Plates on a Circular Cylinder," 27th International Conference on Offshore Mechanical and Arctic Engineering, *OMAE2008*, Estoril, Portugal, June 15–20.
- [11] Assi, G. R. S., and Bearman, P. W., 2009, "VIV and WIV Suppression With Parallel Control Plates on a Pair of Circular Cylinders in Tandem," 28th International Conference on Ocean, Offshore and Arctic Engineering, *OMAE2009*, Honolulu, HI, May 31–June 5.
- [12] Henderson, J., 1978, "Some Towing Problems With Faired Cables," *Ocean Eng.*, **5**, pp. 105–125.
- [13] Wingham, P., 1983, "Comparative Steady State Deep Towing Performance of Bare and Faired Cable Systems," *Ocean Eng.*, **10**, pp. 1–32.
- [14] Packwood, A., 1990, "Performance of Segmented Swept and Unswept Cable Fairings at Low Reynolds Numbers," *Ocean Eng.*, **17**, pp. 393–407.
- [15] Assi, G. R. S., Meneghini, J. R., Aranha, J., Bearman, P. W., and Casaprima, E., 2006, "Experimental Investigation of Flow-Induced Vibration Interference Between Two Circular Cylinders," *J. Fluids Struct.*, **22**, pp. 819–827.
- [16] Freire, C., and Meneghini, J. R., 2010, "Experimental Investigation of VIV on a Circular Cylinder Mounted on an Articulated Elastic Base With Two Degrees-of-Freedom," BBVIV6–IUTAM Symposium on Bluff Body Wakes and Vortex-Induced Vibrations, Capri, Italy.
- [17] Williamson, C., and Govardhan, R., 2004, "Vortex-Induced Vibrations," *Annu. Rev. Fluid Mech.*, **36**, pp. 413–455.